South Otago Coast Sediment Transport: Numerical Modelling

Prepared for:

DUNEDIN CITY COUNCIL | kaunihera a-rohe o Ōtepoti

eCoast
eTakutai

MOHIO - AUAHA - TAUTOKO
UNDERSTAND - INNOVATE - SUSTAIN

PO Box 151, Raglan 3225, New Zealand
Ph: +64 7 825 0087 | info@ecoast.co.nz | www.ecoast.co.nz

South Otago Coast Sediment Transport: Numerical Modelling

Report Status

Version	Date	Status	Approved by
V1	19 Aug 2020	Draft for Client Review	SDG
V2	4 September 2020	Updated Draft for Client Review	EAA
V3	16 September 2020	Approved for Release	EAA

It is the responsibility of the reader to verify the version number of this report.

Authors

Edward Atkin, *HND, MSc (Hons)*

Shaw Mead, *BSc, MSc (Hons), PhD*

Sam O'Neill, *BSc, MSc*

Contents

Figures

Tables

1 Introduction

This report represents one of several pieces of work commissioned by the Dunedin City Council (DCC), which are being undertaken to develop a Coastal Plan for the St Clair to St Kilda coast (Figure 1.1). While the St Clair to St Kilda coast is the focus of the overarching project, an understanding of the larger coastal sediment transport system is imperative, not only to inform decision making in the development of the St Clair to St Kilda Coastal Plan, but also support public consultation. This project considers coastal sediment transport along the southern Otago Coast from Tokatā (Nugget) Point to Kaimata (Cape Saunders) (Figure 1.1).

This report is preceded by a literature review that provides additional detail for the same study site (Atkin *et al.*, 2020), and has been undertaken following a Synopsis of Understanding for the St Clair to St Kilda beach system (Serrano, 2019), that identified a gap in the current understanding of the larger sediment transport system in which St Clair to St Kilda beach sits. This report summarises numerical modelling undertaken to further understand the sediment transport regime along the southern Otago coast. This has been achieved by constructing an uncalibrated long-term wave climate model, and post processing the data to infer inner Depth of Closure, develop boundary conditions; and, implement modelling of longshore sediment transport flux.

1.1 Study Site

The coastal area from Tokatā Point to Kaimata (~110 km of coastline) comprises Molyneux Bay to the south and Taieri Bight in the north, divided by Quoin Point. The shoreline is characterised by sandy beaches backed by dunes, and delineated alongshore by exposed cliffs and headlands, with rocky reefs scattered along the shoreline. The modern sand facies described by Carter *et al.* (1985) is light olive-grey, fine-very fine, moderately to well sorted with a mean grain size of 0.088 - 0.23 mm. Hodgson (1966) and Dyer (1994) report mean grain sizes for St Clair to St Kilda coast of 0.26 mm and 0.30 mm, respectively. Hodgson (1966) also reports median grain sizes of 0.24 mm and 0.26 mm for Sandfly Bay and Allens Beach.

Sediment transport is predominantly south to north. Temporary reversals in the sediment transport system do occur (Carter *et al.*, 1986; Smith, 2007); transport to the south also occurs locally at Tokatā Point. This southerly transport is associated with a circulation of water, or anticyclonic mesoscale eddy, that occurs adjacent to Tokatā Point. The Clutha River is by far the largest source of sand and gravel for the Otago coastline. Associated with this is the modern sand wedge (Carter and Carter, 1986), an extensive “store” in the south Otago

sediment transport system (see Atkin et al., 2020 and references therein). This is a large body of sand that extends from Tokatā Point, where the sand is ~35 m thick, to the north where the width and thickness of the sand store diminish (Figure 1.1).

Sediment budgets were developed by Smith (2007) and T&T (2000), both of which leverage the earlier work of Carter (1986), and Smith (1999; 2000a,b). In terms of material moving through the sediment transport system, from Tokatā Point to Karitane, Smith (2007) quotes Gibb's (1973) sediment flux of 588,888 m^3yr^{-1}. Carter *et al*. (1985) quotes Kirk (1980) at 450,000 m^3yr^{-1} and Gibb (1979) at 1,000,000 m^3yr^{-1}. Johnson *et al*. (2010) estimated an approximate sediment transport flux for the St Clair to St Kilda embayment of 200,000 m^3yr^{-1}

1.2 Depth of Closure

The depth along a beach profile at which sediment transport becomes negligible or ceases is referred to as the Depth of Closure (*DC*). The theoretical concept of *DC* was developed by Hallermeier (1981) and has been used for coastal engineering design, particularly for nourishment projects. *DC* is a function of both wave height and period. *DC* calculations use the effective wave height, that is the wave conditions that are exceeded for 12 hours per year, or with a yearly occurrence probability exceedance of 0.137%. Hallermeier's (1981) equation for *DC* is:

$$DC = 2.28H_s - 68.5\left(\frac{{H_s}^2}{gT^2}\right) \quad [1]$$

where, H_s is the effective wave height, T is the associated weave period and g is acceleration due to gravity.

1.3 Longshore Sediment Transport

Beach morphology is subject to a multitude of processes and drivers. One of the most prominent drivers though, especially on open coast settings, is Longshore Sediment Transport (LST). LST most readily occurs where waves break obliquely to the shore, but also where there are alongshore wave height gradients; both of which set up a longshore current. The dependency of waves for this process means estimations of LST are firmly based on wave climate. There are a range of models and approaches to estimating LST dating back to the early 1980's.

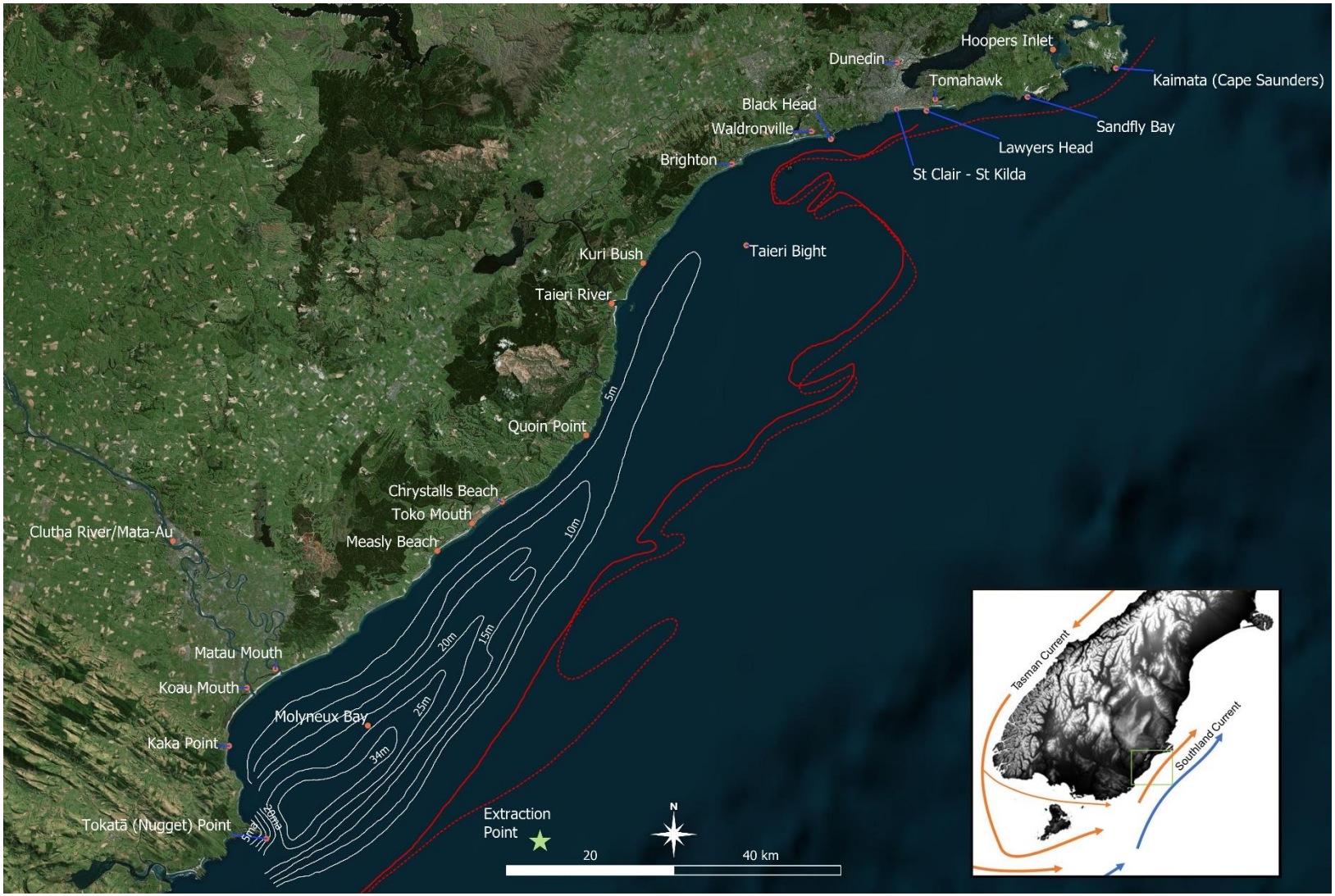

Figure 1.1. Annotated aerial photo showing: the depth of material in the modern sand wedge of Carter and Carter (1986 - white lines); the seaward limit of the modern sand facies (Carter *et al*., 1985 (dashed red line); Carter and Carter, 1986 (solid redline)); offshore wave climate time series extraction point (white dot); and prominent locations within the study site. Insert: illustration of the Tasman and Southland Currents around the southern tip of the South Island of New Zealand, and approximate study site (green box).

Mils-Homens *et al*. (2013) and Fernández-Fernández *et al*. (2016) provide comparisons of LST equations, with the former providing what is known as the modified-Kamphuis (after Kamphuis, 1991) formula:

$$LST = 0.15{\rho_s}^{a}\left(\frac{{H_{sb}}^{2.75}{T_p}^{0.89}{m_b}^{0.86}{d_{50}}^{-0.69}\sin(2\theta_b)^{0.5}}{(\rho_s-\rho)(1-a)}\right) \text{ [2]}$$

where: *LST* is volume per unit time in m^3s^{-1}; H_{sb} is the significant wave height at the breaker line, T_p is associated peak period; m_b is the beach slope from the breaking line to the shoreline; d_{50} is median sediment grain size; θb is angle between the wave crests and the shoreline at the breaker line; ρ_s is the density of the sediment; ρ the density of the water; and a is the porosity index (Van Rijn, 2014). The modified-Kamphuis methodology was applied to this investigation. This study is not estimating cross shore sediment transport.

2 Methodology

2.1 Bathymetry

In order to numerically model waves and post process model output, seafloor depths across the area of interest, or bathymetry, is required. The bathymetric data set used in this study comprises Land Information New Zealand's (LINZ) nautical chart and GEBCO (Becker *et al*., 2009) data. These datasets were validated against two sets of survey data, one from Molyneux Bay (Williams and Goldsmith, 2014.) and another from south Dunedin (Johnson *et al*., 2010). All bathymetric datasets were referenced to Mean Sea Level (MSL).

2.2 Transects

To present metrics along the length of the coastline of the study site, LINZ 1:50,000 coastline, which approximates MSL, was discretised at 250 m. At each discretised point, a transect that is perpendicular to the orientation of the coast was constructed. The orientation of the coast was represented by the mean of the orientation of the coastline 50 m either side of the discretized point. The shore normal transects were extended inland to the point at which the profile height reached ~3 m above MSL. The offshore extent of each transect is a function of depth, with the end point approximating 20 m deep MSL. A depth of 20 m was used as a first pass value for *DC* (Section 1.2), which was based on an estimate of the outer *DC* (offshore limit for *DC*) using mean conditions from the offshore wave climate (Hallermeier, 1981). Figure 2.1 presents the transects. Some transects were omitted because of their orientation, resulting from the dendritic nature of the South Otago coastline, which meant that calculation of any metric based on these transect would yield poor, unusable results. The areas where transects were omitted were almost entirely associated with the longer headlands that are oblique or perpendicular to the general orientation of the coast.

2.3 Wave Modelling

An industry-standard wave model, SWAN (Simulating WAves Nearshore), incorporating the generation, propagation, and transformation of wave fields in both deep water and nearshore regions was used to simulate wave conditions at the study site. The SWAN model solves the spectral action density balance equation for frequency-directional spectra. This means that the growth, refraction, and decay of each component of the complete sea state, each with a specific frequency and direction, is solved, giving a comprehensive description of the wave field as it changes in time and space (Holthuijsen *et al*., 2004).

Numerical model domains were constructed by interpolating latitudinal, longitudinal and depth/elevation (XYZ), data on to rectilinear grids. The XYZ data used to construct gridded domains is described in Section 2.1. The modelling framework employs a nesting scheme to increase the spatial resolution at the study sites and areas of interest. On a New Zealand scale grid with a horizontal resolution of 0.05° (Figure 2.2), a 41-year wave hindcast was simulated. The model boundary conditions consisted of the European Centre for Medium-Range Weather Forecast's (ECMWF) ERA5 2-dimensional wave spectra with a horizontal resolution of 0.5° (Hersbach, *et al*., 2020), and 10 m wind data sourced from the National Centre for Environmental Prediction's (NCEP) hourly global reanalysis model (Kalnay *et al*., 1996) with a spatial resolution of 0.312°.

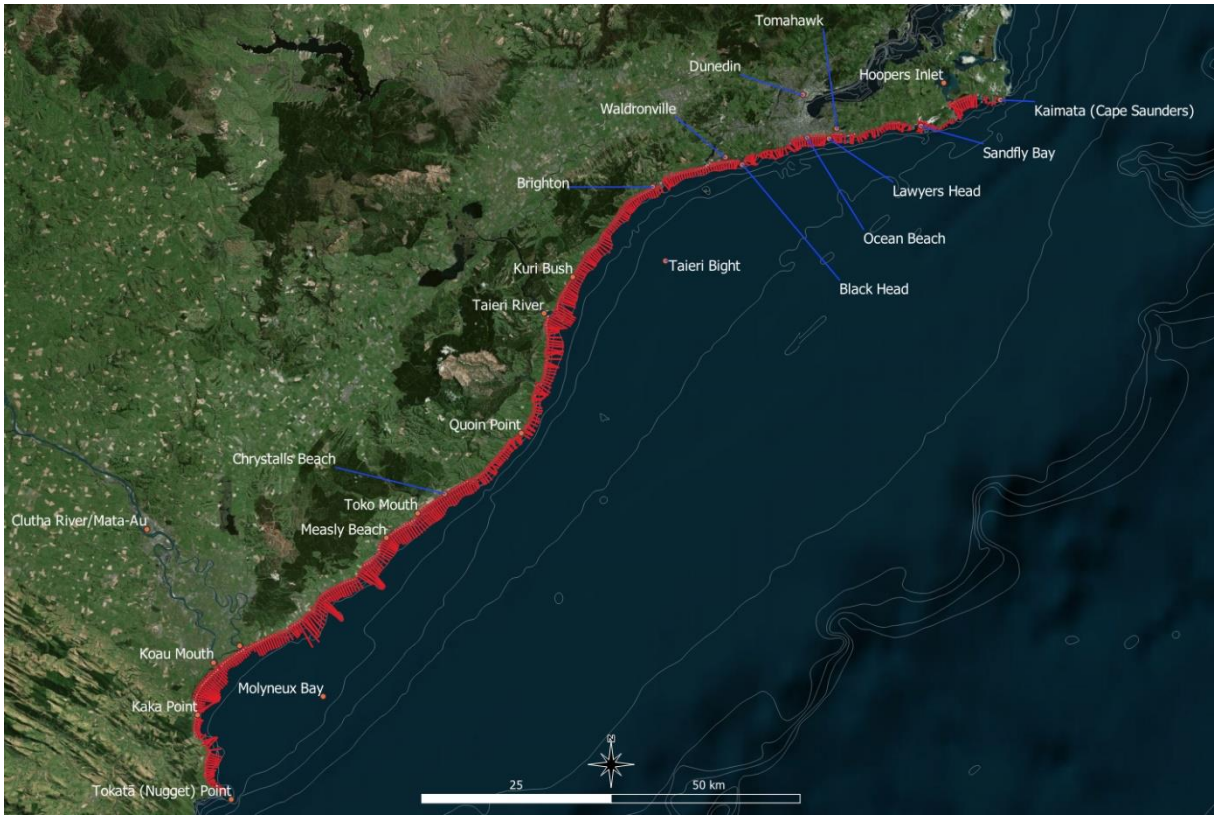

Figure 2.1: Transect locations (red lines) at 250 m intervals along the coast.

Nested within the New Zealand scale domain was a 2nd level sub-regional scale domain, with a spatial resolution of 500 m (Figure 2.2). Within the 2nd level nest are 3 local nests with 100 m resolution. The local nests, A, B and C, cover from Tokatā Point to Quoin Point, Quoin Point to Brighton, and Bright to Kaimata, repsectively. Characterised boundary conditions for each of the level 3 nested grids were constructed from a time series extracted from the level 1 hindcast at discrete locations on the boundary of the level 2 nest (Figure 2.2).

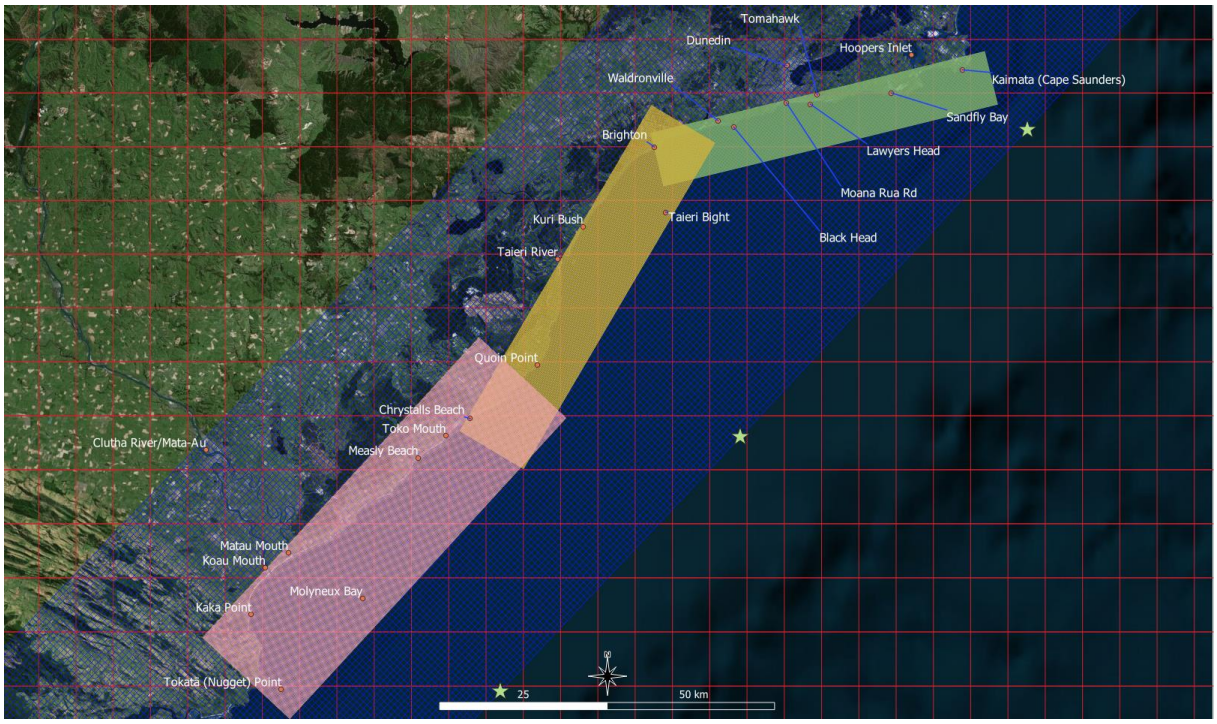

Figure 2.2: Model domains (grids). Red: course resolution NZ scale mode; blue: 500 m sub regional grid; pink (A grid), orange (B grid) and green (C grid), 100 m resolution local grids. With representative wave conditions extract points (green stars).

2.3.1 Sub-regional Boundary Conditions

Two sets of sub-regional boundary conditions were constructed. One for *DC* estimation and another for the purpose of sediment transport modelling. Boundary conditions for *DC* estimations were developed from the long term wave climate data extracted from the 3 representative wave condition extraction points (Figure 2.2) as follows:

- For each year with in the 41-year hindcast, the wave climate timeseries was divided based on wave direction into 30° bins from 50°N to 230°N.
- For each year and each bin, the instances of effective wave height, or significant wave height exceeded only 12 hours out of a single year, or the greatest 0.137% waves in a year (Brutsché *et al* 2016, Hallermeier, 1981) were identified. These instances, along with coincident wave periods and directions were then averaged.
- An additional boundary condition for each direction bin was constructed using all 41 years of data.

The result is 252 boundary conditions. Sediment transport modelling boundary conditions were developed at each of the 3 representative nodes as follows:

- The 41-year time series was binned in both wave direction and height. Directional bins were 15° wide from 0 to 359.99°. Wave height bins were 0.5 m wide ranging from 0 m to 8 m.
- To provide a more accurate representative set of conditions for each bin, wave height, period and direction populations of each bin were averaged (as opposed to traditional approach of using the bin centres).
- An occurrence weighting was assigned to each bin based on the bin's population.

Table 2.1 through Table 2.3 present the results of this process, which provides 154, 141 and 147 weighted wave conditions for level 3 nested grids A, B and C, respectively. Each characterised wave condition for both *DC* and sediment transport regime was propagated from the offshore edge of the level 2 nest, and through the local level 3 nest.

Table 2.1: Binned and weighted wave climate for the grid A.

Wave Direction (°T) \ Wave Height (m)	0.0-0.5	0.5-1.0	1.0-1.5	1.5-2.0	2.0-2.5	2.5-3.0	3.0-3.5	3.5-4.0	4.0-4.5	4.5-5.0	5.0-5.5	5.5-6.0	6.0-6.5	6.5-7.0	7.0-7.5	7.5-8.0
345-360																
330-345																
315-330																
300-315																
285-300																
270-285																
255-270																
240-255																
225-240			0.004	0.009	0.003	0.006	0.002		0.001							
210-225	0.001	0.333	2.361	3.680	3.311	2.311	1.494	0.841	0.469	0.249	0.104	0.046	0.020	0.005		
195-210	0.010	1.344	6.287	7.190	5.199	3.077	1.587	0.882	0.450	0.230	0.105	0.058	0.029	0.013	0.008	0.001
180-195	0.014	1.347	4.746	4.271	2.442	1.110	0.496	0.227	0.114	0.036	0.013	0.016	0.003	0.001	0.001	
165-180	0.007	1.085	3.253	2.363	1.082	0.450	0.181	0.057	0.046	0.018	0.004	0.003	0.004			
150-165	0.003	0.796	2.372	1.660	0.726	0.249	0.094	0.043	0.024	0.009	0.003	0.003	0.002			
135-150	0.004	0.597	1.975	1.523	0.572	0.224	0.073	0.033	0.013	0.004	0.002	0.003	0.001	0.001		
120-135	0.001	0.471	1.850	1.494	0.648	0.183	0.081	0.030	0.015	0.002	0.001					
105-120	0.001	0.483	1.894	1.693	0.670	0.252	0.078	0.031	0.011	0.004	0.002	0.003	0.002			
90-105		0.426	2.006	1.747	0.754	0.237	0.081	0.022	0.007	0.006	0.004	0.003	0.002	0.003	0.002	
75-90		0.441	1.890	2.005	0.834	0.279	0.088	0.039	0.013	0.006	0.001	0.001				
60-75		0.204	0.968	1.026	0.525	0.224	0.081	0.023	0.013	0.003	0.001	0.001				
45-60		0.003	0.011	0.005												
30-45																
15-30																
0-15																

% Occ: 7, 6, 5, 4, 3, 2, 1

2.4 Depth of Closure

The numerical model outputted waves statistics across the nested grids. In this case, output was created for each of the 6 directional bins for each year. For each output, the wave height and period were interpolated at 1 m intervals along the length of each of the shore normal transects. Using the wave height and period from each interpolated point the *DC* was calculated (Eq. 1). The *DC* for each transect, under each of the simulated wave conditions, is the point at which the depth profile and *DC* along each transect intersect or converge (e.g. Kang *et al.*, 2018). An example of this is Figure 2.3.

Table 2.2: Binned and weighted wave climate for the grid B.

Wave Direction (°T) \ Wave Height (m)	0.0-0.5	0.5-1.0	1.0-1.5	1.5-2.0	2.0-2.5	2.5-3.0	3.0-3.5	3.5-4.0	4.0-4.5	4.5-5.0	5.0-5.5	5.5-6.0	6.0-6.5	6.5-7.0	7.0-7.5	7.5-8.0
345-360																
330-345																
315-330																
300-315																
285-300																
270-285																
255-270																
240-255																
225-240																
210-225		0.095	0.708	1.041	0.861	0.552	0.300	0.139	0.062	0.025	0.008	0.001				
195-210	0.008	1.208	5.532	6.917	5.184	2.992	1.625	0.922	0.471	0.222	0.105	0.047	0.017	0.006		
180-195	0.009	1.793	6.079	5.547	3.037	1.515	0.638	0.315	0.115	0.047	0.026	0.009	0.002	0.002	0.002	
165-180	0.023	1.572	4.009	2.880	1.206	0.437	0.168	0.071	0.048	0.009	0.006	0.003	0.003			
150-165	0.012	1.306	2.897	1.780	0.707	0.248	0.103	0.047	0.024	0.008	0.003	0.004	0.001			
135-150	0.008	1.032	2.421	1.570	0.532	0.221	0.075	0.032	0.019	0.006	0.002	0.003	0.001			
120-135	0.003	0.866	2.413	1.546	0.622	0.136	0.074	0.028	0.013	0.001	0.002					
105-120	0.008	0.791	2.434	1.786	0.669	0.221	0.067	0.021	0.011	0.005	0.002	0.003	0.001			
90-105		0.713	2.489	1.855	0.667	0.188	0.073	0.028	0.008	0.005	0.003	0.003	0.002	0.004		
75-90		0.666	2.527	2.146	0.814	0.252	0.061	0.043	0.009	0.004	0.001	0.001				
60-75		0.325	1.367	1.285	0.658	0.237	0.080	0.027	0.011	0.003		0.001				
45-60		0.003	0.027	0.015	0.004											
30-45																
15-30																
0-15																

% Occ: 1 2 3 4 5 6

Table 2.3: Binned and weighted wave climate for the grid C.

Wave Direction (°T) \ Wave Height (m)	0.0-0.5	0.5-1.0	1.0-1.5	1.5-2.0	2.0-2.5	2.5-3.0	3.0-3.5	3.5-4.0	4.0-4.5	4.5-5.0	5.0-5.5	5.5-6.0	6.0-6.5	6.5-7.0	7.0-7.5	7.5-8.0
345-360																
330-345																
315-330																
300-315																
285-300																
270-285																
255-270																
240-255																
225-240																
210-225		0.053	0.429	0.540	0.473	0.344	0.218	0.119	0.057	0.031	0.010	0.002				
195-210	0.003	0.971	4.795	6.442	5.012	2.998	1.632	1.004	0.532	0.279	0.139	0.060	0.026	0.006	0.001	0.002
180-195	0.007	1.423	5.494	5.509	3.200	1.624	0.696	0.310	0.154	0.058	0.028	0.015	0.007	0.002	0.001	
165-180	0.010	1.363	3.843	2.934	1.293	0.486	0.177	0.072	0.051	0.017	0.008	0.004	0.003			
150-165	0.018	1.125	2.816	1.790	0.773	0.275	0.118	0.061	0.030	0.013	0.004	0.003	0.003			
135-150	0.008	0.934	2.322	1.544	0.583	0.215	0.083	0.031	0.028	0.009	0.003	0.002				
120-135	0.008	0.844	2.328	1.542	0.593	0.200	0.085	0.029	0.019	0.006	0.002					
105-120	0.003	0.801	2.374	1.736	0.714	0.224	0.083	0.027	0.013	0.004	0.002	0.003				
90-105	0.001	0.715	2.442	1.858	0.774	0.255	0.073	0.037	0.013	0.008	0.003	0.003	0.003	0.003		
75-90		0.683	2.514	2.297	0.933	0.252	0.068	0.034	0.015	0.006	0.001					
60-75		0.471	2.165	2.230	1.172	0.533	0.185	0.058	0.020	0.007	0.003	0.003				
45-60		0.033	0.194	0.276	0.157	0.063	0.028	0.010	0.005	0.003						
30-45																
15-30																
0-15																

% Occ: 1 2 3 4 5 6

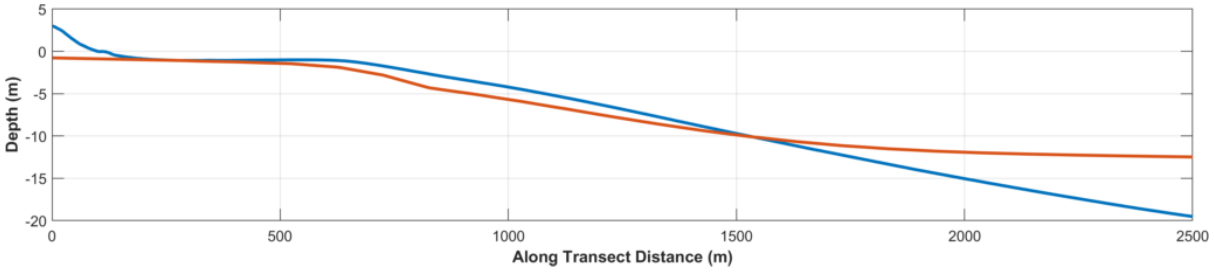

Figure 2.3: Convergence of transect depth profile (blue line) and *DC* values (red line) during storm conditions (~6 m at 12 s).

A final *DC* for each year (and in the long-term case, using the whole 41-year time series) was taken as the deepest value from the 6 directional bins. From the 41-year *DC* values, statistics of maximum, minimum, standard deviation, and range of *DC*, at each transect were calculated.

2.5 Sediment Transport

For each shore-normal transect, at the location of the maximum *DC* (from Section 2.4), the transformed weighted wave conditions (Section 2.3.1) were extracted. The occurrence weighted conditions provided the boundary condition for 1-dimensional sediment transport modelling. The depth along the transect, interpolated at 1 m intervals, provided the model domain.

The modified-Kamphuis longshore sediment transport model (based on Mil-Homens *et al.*, 2013) predicts refraction and shoaling, breakpoint wave conditions and estimates longshore sediment transport on open coasts. Tuneable parameters in the sediment transport model include sediment grain size (D_{50}), and sediment density (ρ_s). The sensitivity of these tuneable parameters was explored for 2 transects in each level 3 nest. The transects were selected to account for a range in exposure and seabed slope.

Values for D_{50} in the study site are reported as 0.088-0.30 mm (Carter *et al*., 1985; Hodgson, 1966; Dyer, 1994). This range encompass very fine sand, which is likely to be a small fraction of in the sediment distribution. The upper (Dyer, 1994) and lower (Carter *et al.*, 1985) reported limits of 0.23 mm and 0.3 mm and a mean of 0.265 are used in sensitivity testing. Sediment densities can vary greatly based on the geological setting and a value of 2670 kgm^{-3} is often assumed. Godfrey *et al.* (2001) report Haast Schist densities from 2682 kgm^{-3} to 2738 kgm^{-3}. Tenzer *et al.* (2010) report a mean Schist value of 2732 kgm^{-3}. Sensitivity testing included ρ_s values of 2670, 2704 and 2738 kgm^{-3}.

The sediment transport locations (each transect) were filtered to remove all locations when the sediment transport equations were not applicable. These locations included the rocky and cliff lined shores where longshore sand transport within the surf zone is more complex than the equations can account for, and locations where the transect is highly oblique to the bathymetric isobaths and/or the wave climate.

3 Results

3.1 Depth of Closure

The maximum and minimum *DC* are presented in Figure 3.1 through Figure 3.4. *DC* ranges from 2 to 15 m. The shallowest *DC* values are associated with the sheltered bays close to Kaka Point. These points also have the lowest ranges in *DC* across the 41 years. The deepest *DC* values are located toward the more exposed eastern end of Kaimata, with ranges of ~6 m (study site maximum); range in *DC* is also large between Quoin Point and Taieri.

There is a general trend of increasing *DC* from Tokatā Point to Kaimata. Maximum *DC* values from ~Toko Mouth toward Kaimata are generally greater than 10 m. The mean range of *DC* around the South Dunedin coast is ~4 m, indicating a moderate amount of interannual variability. In Figure 3.1 *DC* locations are largely removed from the hashed polygon, which represented the 5 m depth of material in the modern sand wedge (Carter and Carter, 1986).

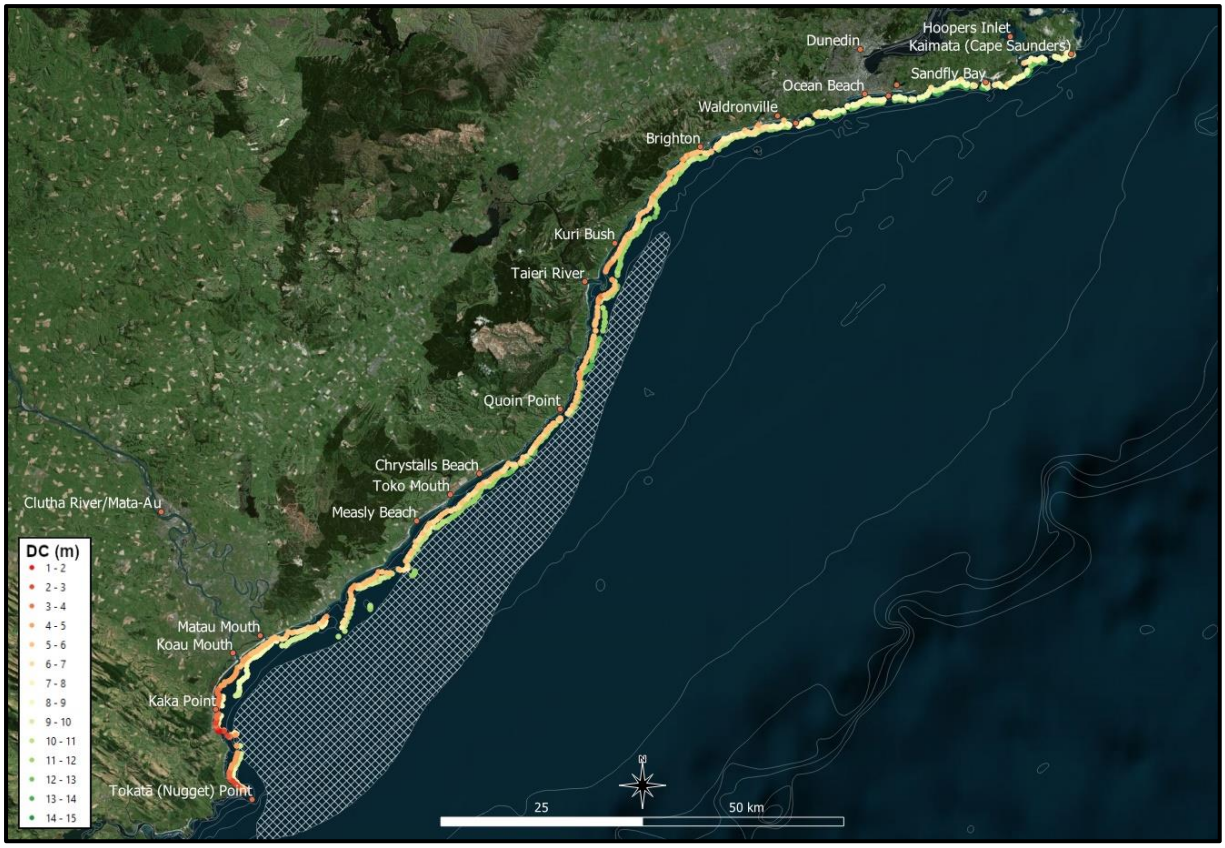

Figure 3.1: Tokatā Point to Kaimata: *DC* minima and maxima for each transect location (coloured circles), and 5 m depth of material polygon in the modern sand wedge.

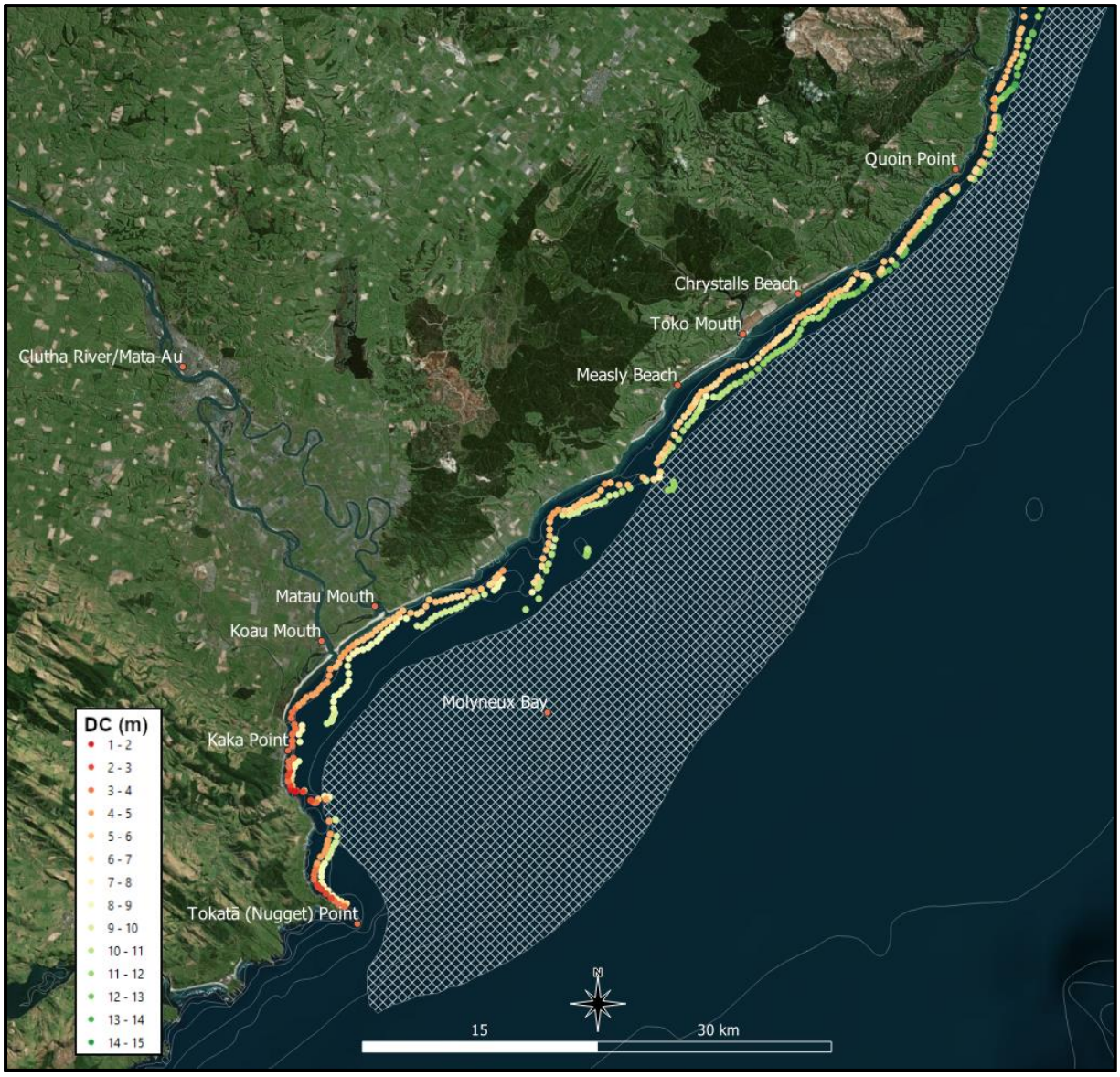

Figure 3.2: Tokatā Point to Measley Beach: *DC* minima and maxima for each transect location (coloured circles), and 5 m depth of material polygon in the modern sand wedge.

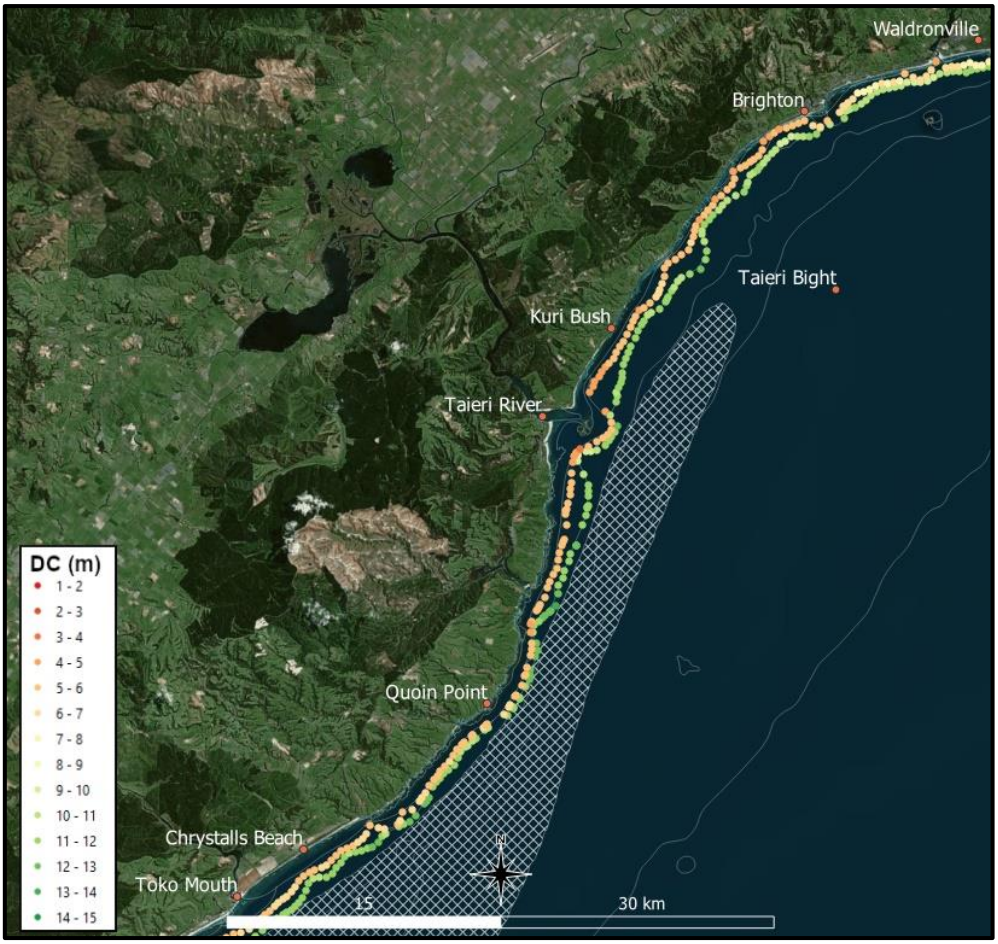

Figure 3.3: Toko Mouth to Waldronvile: *DC* minima and maxima for each transect location (coloured circles), and 5 m depth of material polygon in the modern sand wedge.

Figure 3.4: Brighton to Kaimata: *DC* minima and maxima for each transect location (coloured circles), and 5 m depth of material polygon in the modern sand wedge.

3.2 Sediment Transport

Sediment transport results are presented as positive and negative potential sediment transport flux. In this study, sediment transport toward Kaimata is positive and sediment transport

toward Tokatā is negative. The main metric presented is **net** sediment transport potential, i.e. the positive transport potential weighed against the negative.

3.2.1 Sensitivity tests

Figure 3.5 presents the results from the sensitivity tests. The tests show that the percentage difference between the tested variables is the same at each transect. Noting the transect locations have different seabed slopes and wave climates. Altering the sediment grain size (D_{50}) by a standard deviation of the reported range results in 10% and 8% differences in transport potential for a grainsize decrease and increase, respectively. For an increase and decrease of 34 kgm^{-3} in sediment density (ρ_s), the difference is 1% and 2%, respectively. This indicates ρ_s has a smaller impact than sediment grain size on the outputs of the modified-Kamphuis sediment transport model. The relationships are as expected (e.g. increased grain size results in reduced sediment transport). The magnitude of potential error (up to 12%) is not excessive and provides confidence in other components of the sediment transport model (e.g. wave transformation, estimation of seabed slope). Given the scale of the study site a potential error of this magnitude is considered acceptable. The mean values (0.265 mm and 2704 kgm^{-3}) were used in the results for all transects.

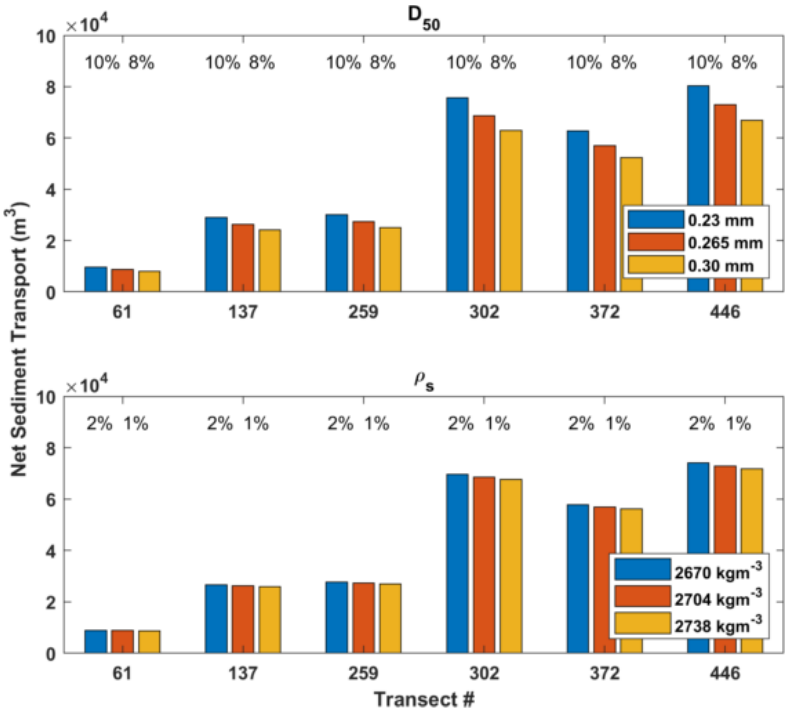

Figure 3.5: Sediment transport potential sensitivity for D_{50} (top) and ρ_s (bottom) for 6 different transects, 2 from each 3rd level nest. Values at the top of each plot indicate the percentage difference between tests.

3.2.2 Tokatā Point to Kaimata

Mean and maximum sediment transport rates over the entire study area are provided in Table 3.1. The positive net value agrees with the predominant south to north sediment transport system reported by various authors. The maximum values for sediment transport potential estimated in this study are on the same order of magnitude as those reported in previous work (588,888 m^3yr^{-1}: Gibb, 1973 cited in Smith, 2007; and 450,000 m^3yr^{-1} to 1,000,000 m^3yr^{-1}: Gibb, 1979; Kirk, 1980; Carter *et al*., 1985), although less by several 100,000 m^3yr^{-1}. Figure 3.6 provides a geographical overview of the sediment transport potential. Figure 3.7 through Figure 3.10 present this data in bar plot format. The reversal of sediment transport around the Clutha River mouth, described in previous studies (Carter *et al*., 1986; Smith, 2007), is apparent.

Table 3.1: Sediment transport potential statistics.

	Mean (m^3yr^{-1})	Maximum (m^3yr^{-1})
Negative Flux	56,651	334,031
Positive Flux	91,159	334,539
Net Transport	34,508	248,464

Net negative sediment transport indicates reversal in direction relative to the overall net transport direction (from Tokatā Point to Kaimata). Prominent reversals occur at Koau Mouth, north of Wangaloa, Brighton, Westwood and Waldronville, Tomahawk Beach and Sandfly Bay. The locations of these reversals are shown in Figure 3.11. Most of the reversals collocate with, or are updrift (net) of headlands, occurring toward the north and/or east end of sandy embayments. At Waldronville, a negative sediment flux occurs in the lee of Green Island, west of the mouth of the Kaikorai Stream (Figure 3.12).

The mean net sediment transport potential between Bruce Rocks and Brighton is ~60,000 (gross ~215,000) m^3yr^{-1}. Between Brighton and Blackhead (i.e. Waldronville Beach) the mean net sediment transport potential is ~7,600 (gross ~108,000) m^3yr^{-1}; and from St Clair Headland to Lawyers Head it is ~40,000 (gross ~115,000) m^3yr^{-1}.

In the St Clair to St Kilda embayment (Figure 3.13), there are 2 transect locations that exhibit reversals in sediment transport. One is adjacent to Moana Rua Rd, and the other at the Lawyers Head end of the beach. The negative net flux at Moana Rua Rd is ~2000 m^3yr^{-1}; which in the scale of potential sediment transport occurring on the south Otago coast, is essentially net zero. Despite this, the gross potential transport is more than 80,000 m^3yr^{-1}, a value not dissimilar from the other positive flux values at other transects along the St Clair to St Kilda embayment.

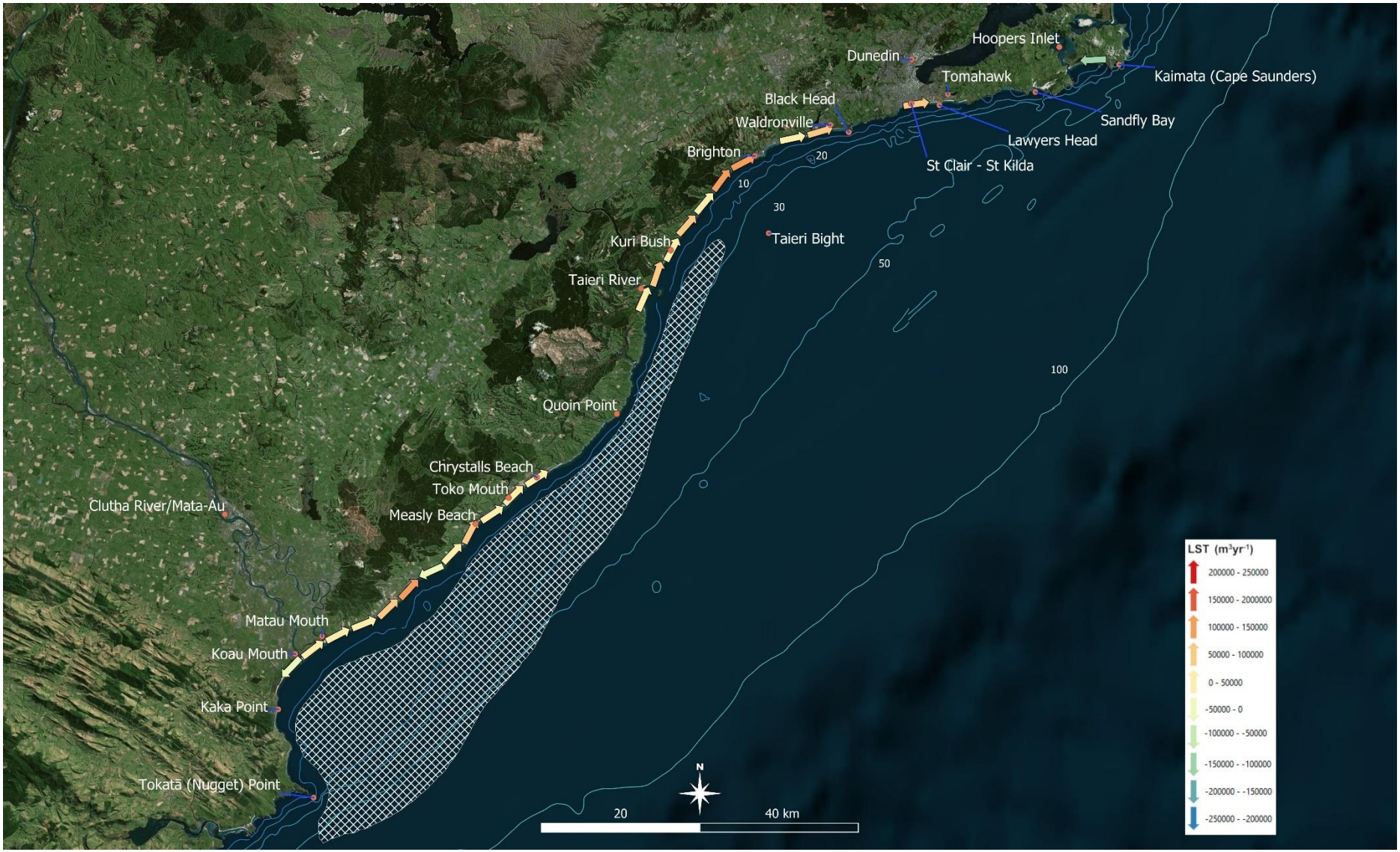

Figure 3.6: Filtered and thinned net sediment transport potential, arrows denoting net transport direction along the South Otago coast.

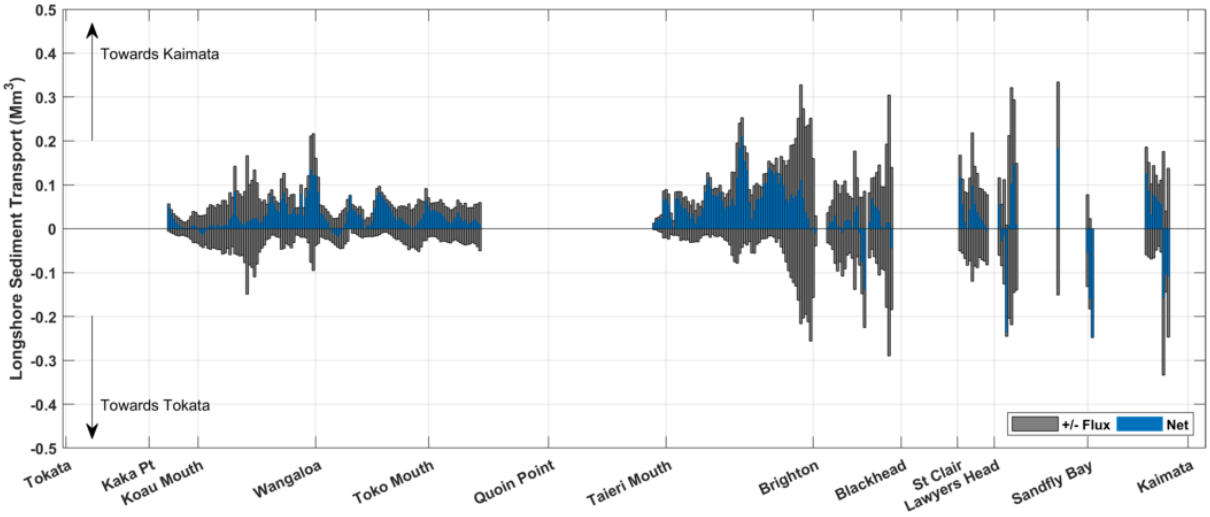

Figure 3.7: Bar plot of potential sediment transport net and flux from Tokatā Point to Kaimata.

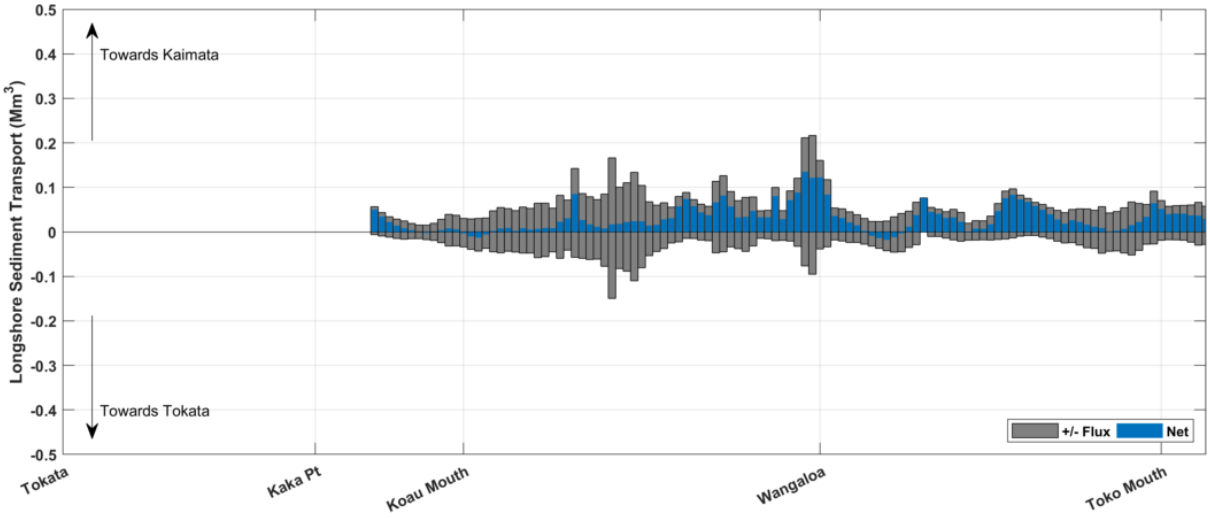

Figure 3.8: Bar plot of potential sediment transport net and flux from Tokatā Point to Toko Mouth.

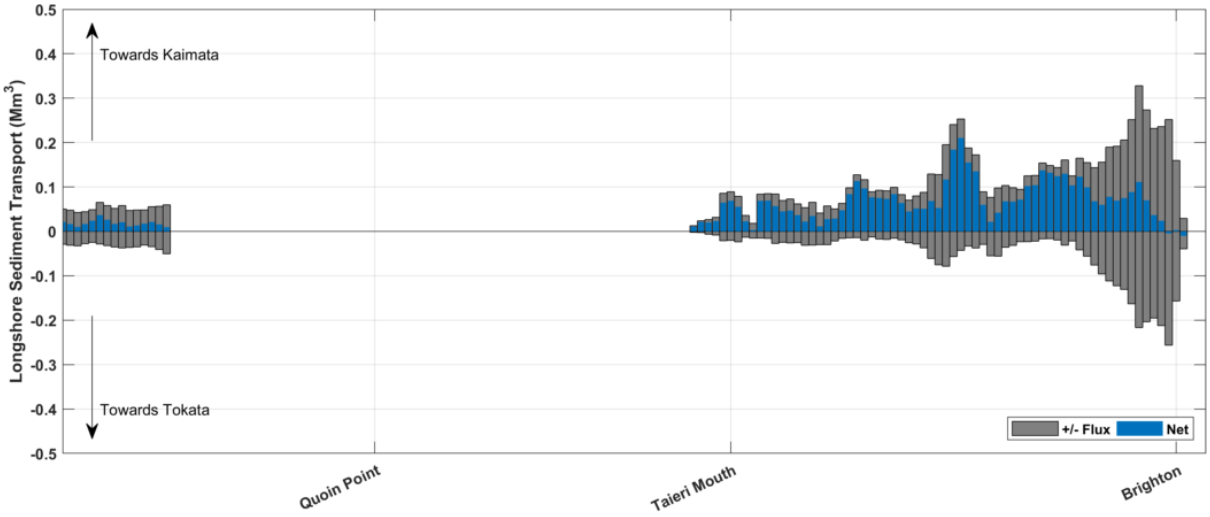

Figure 3.9: Bar plot of potential sediment transport net and flux from Toko Mouth to Brighton.

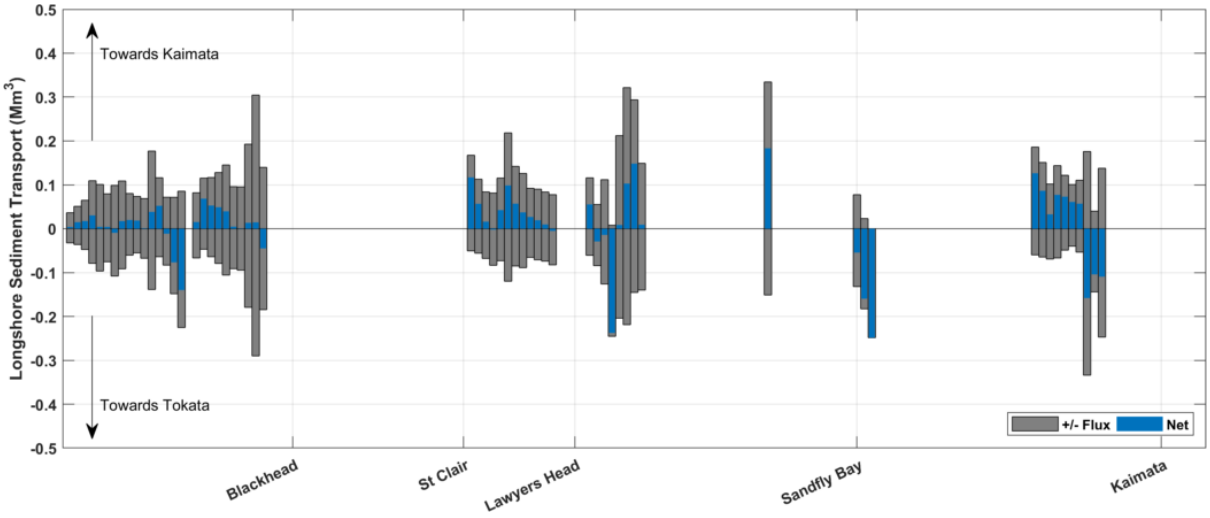

Figure 3.10: Bar plot of potential sediment transport net and flux from Brighton to Kaimata.

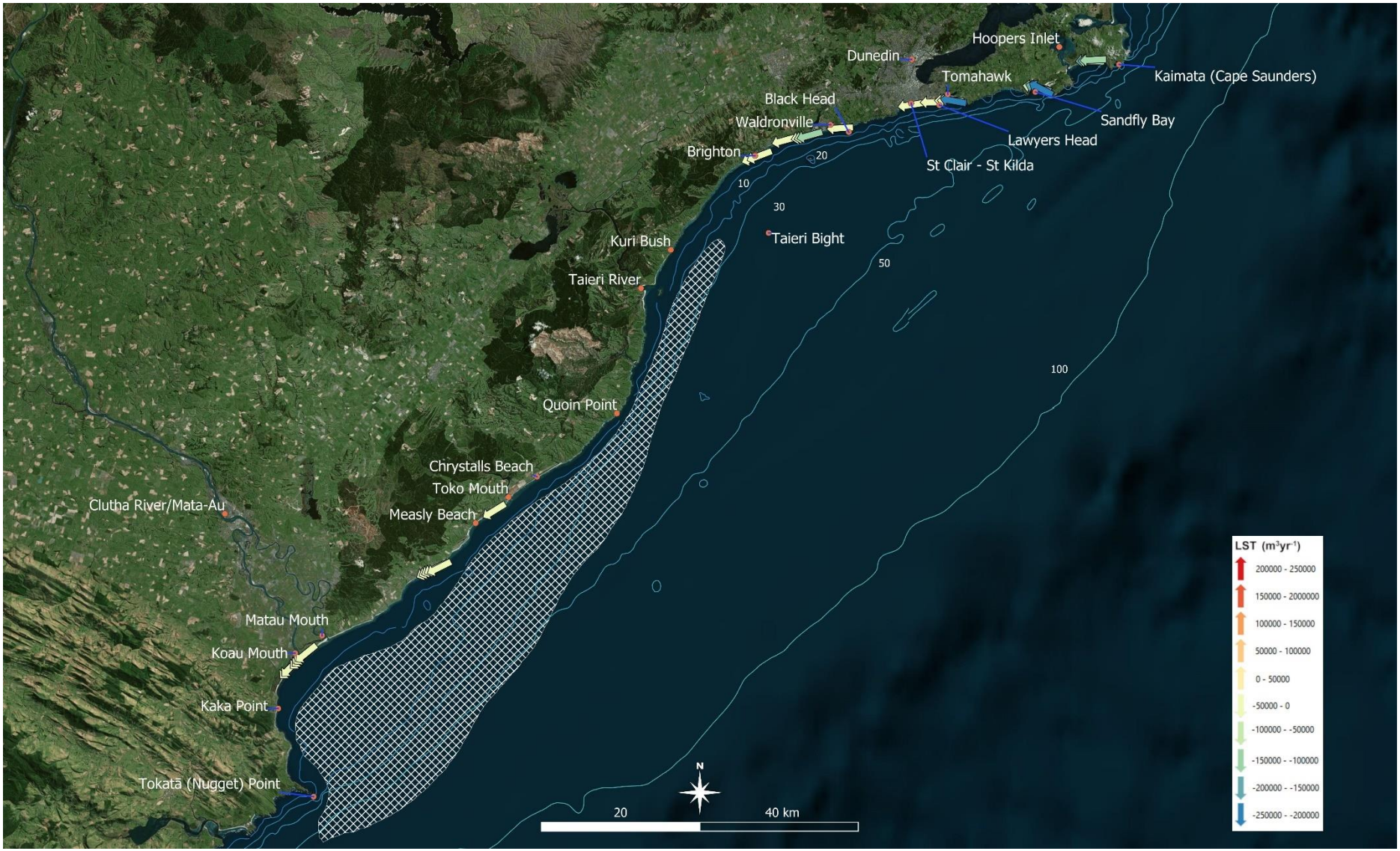

Figure 3.11: Locations of reversals in net sediment transport direction relative to the net transport regime.

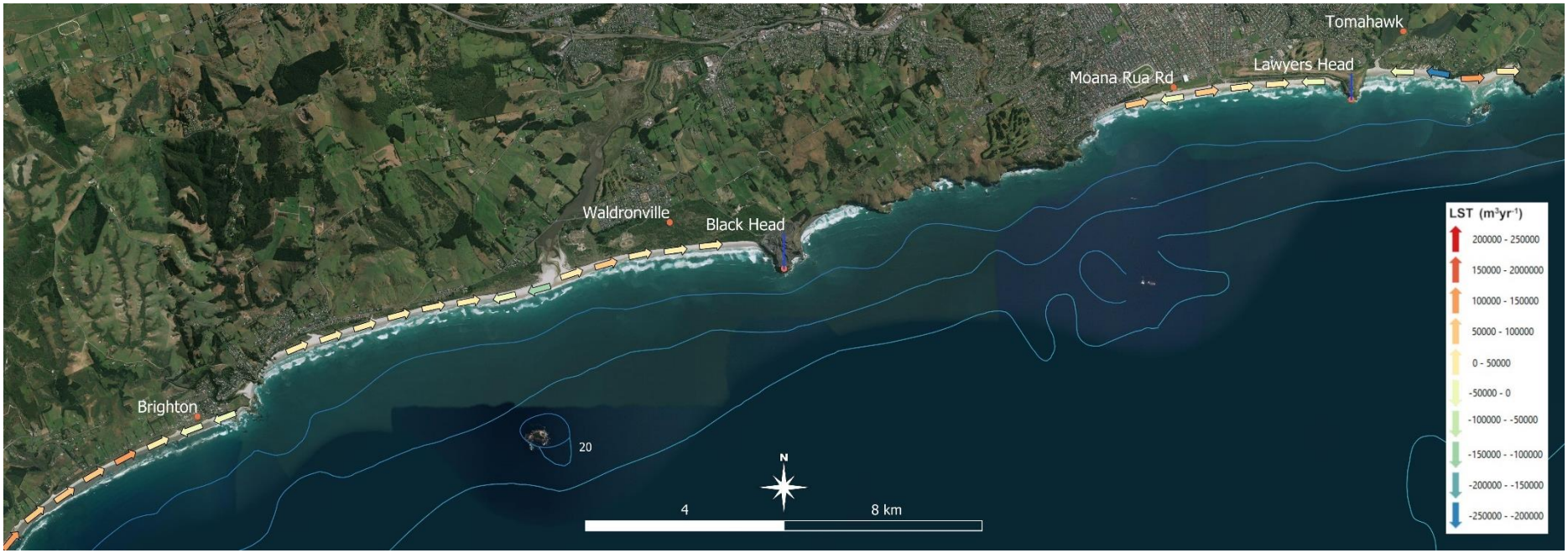

Figure 3.12: Net sediment transport potential between Bruce Rocks and Maori Head, arrows denoting transport direction.

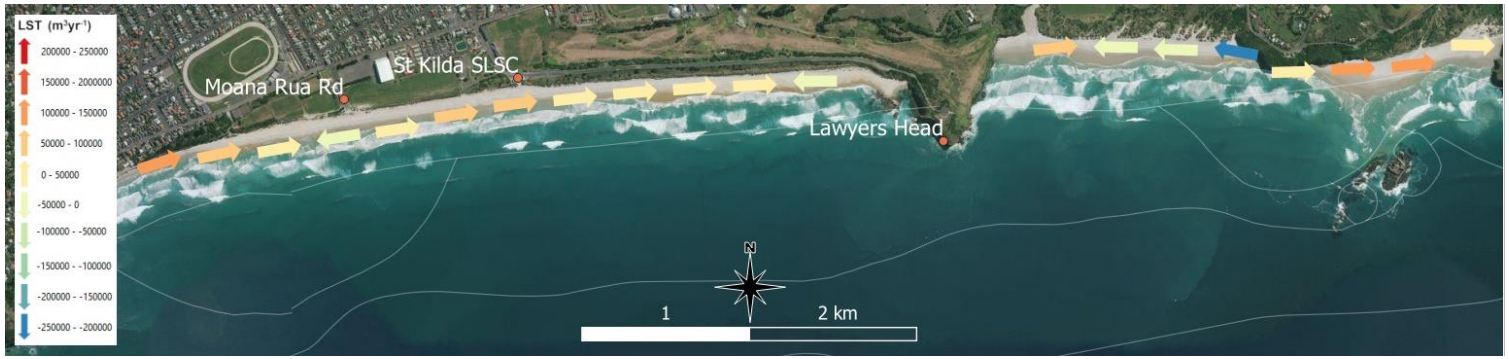

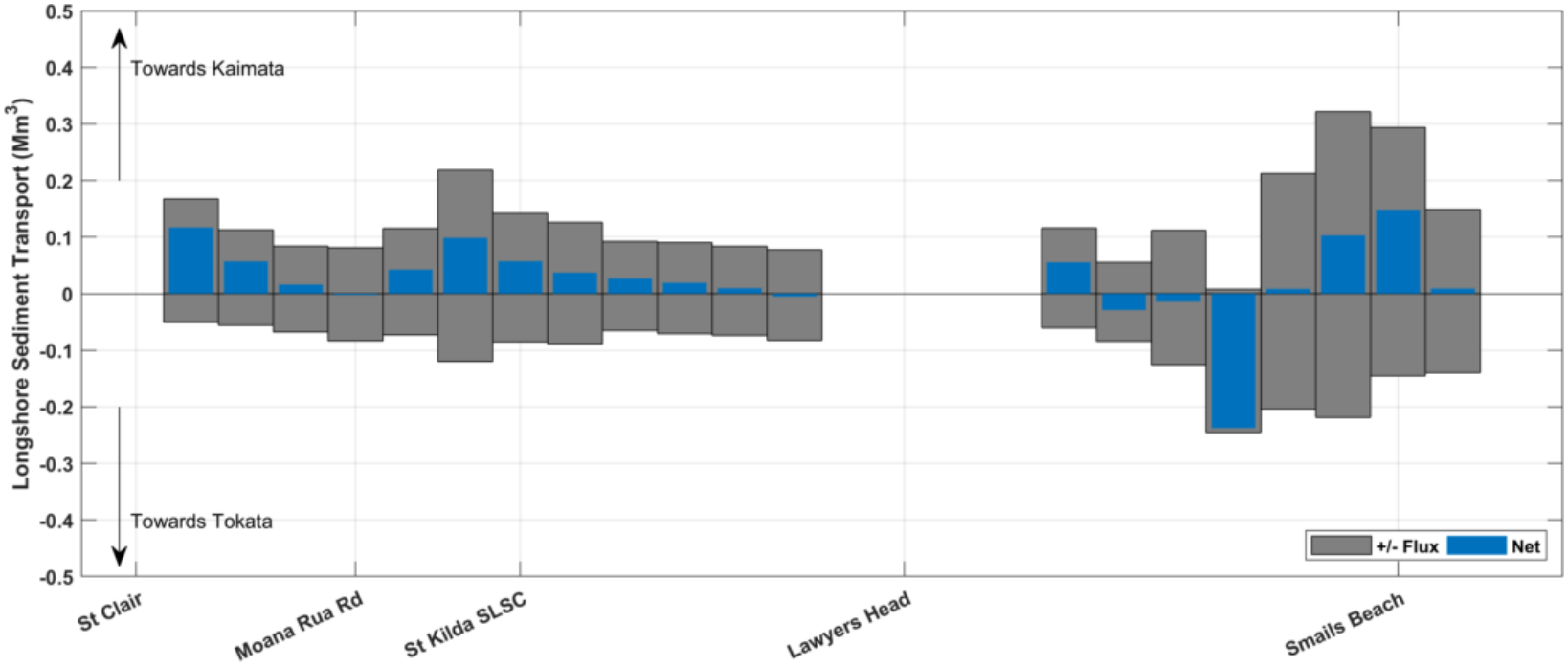

Figure 3.13: Net sediment transport potential between St Clair and Maori Head, arrows denoting transport direction.

4 Discussion

The sand wedge on the south Otago coast contains an exceptionally large volume of material. Whilst the sand wedge likely feeds material to the coastline, the bulk of the sand wedge is located well outside the Depth of Closure (*DC*), meaning that shoreward sediment transport from the bulk of the sand wedge may only occur during extreme events. *DC* generally increases from Tokatā Point to Kaimata, which means the active nearshore zone is much deeper. This reflects the increase in exposure to larger waves from the southern to northern end of the study site. From a management perspective, renourishment volumes are often estimated as a function of *DC.* This would mean that the required renourishment volumes would also increase along the coast. However, *DC* values are relatively consistent across the St Clair to St Kilda coast, indicating little variation in renourishment volumes across the embayment would be required.

The sediment transport potential at the proximal end of the sand wedge (i.e. Tokatā Point) is generally lower compared to the transport rate at the distal end and the area of interest (St Clair/St Kilda). The longshore sediment transport (LST) regime is therefore one of demand potential outstripping supply potential (higher net transport rates and lower transport depths at the distal end). As these beaches are largely sustained along the coast, an obvious assumption is that LST accounts for only a portion of the sediment transport system.

The Taieri River delivers 17,000 to 27,000 m^3yr^{-1} of sand/gravel to the south Otago system (Smith, 2007; T&T, 2000). Mean LST flux around the Taieri River source is ~36,000 m^3yr^{-1}. Comparatively, mean LST flux northeast of Matua Mouth (Clutha River) is ~26,000 m^3yr^{-1}.

At a more local level, it is estimated that the LST flux is reduced through the Waldronville Beach, relative to the net and gross values estimated for the Brighton area and St Clair to St Kilda. If we consider that Waldronville is the source for St Clair, the LST subsystem is in a net deficit.

Figure 4.1 includes the conceptual schematisation of the mean sediment transport during a southerly event theorised by Johnson, *et al*. (2010); who estimated a total sediment flux of ~200,000 m^3yr^{-1}, based on a sediment flux of 500-750 m^3/day (182,500-273,750 m^3yr^{-1}). It should be noted that the concept represents only a snapshot of the processes occurring at the study sites. At the eastern end of the St Clair to St Kilda embayment beach Johnson *et al*. depict a pair of circulation cells. The reversal at the Lawyers Head end of the beach observed in this work collocate with circulation patterns suggested by Johnson *et al*. (2010). The transport pathway from the middle of the beach to the west estimated by Johnson *et al.* is also observed in this work, albeit not to the same extent. The arrows depicting circulation cells and

onshore/offshore driven pathways, which have not been determined as part of this study, were derived from the use of a 2D sediment transport model that is suited to relatively smaller study sites while considering coastal processes in more detail.

The annual sediment transport flux estimate of Johnson *et al*. (2010) is roughly double that of the gross LST estimated in this work. It is likely that this disparity can be at least partially attributed to the cross-shore sediment flux. If this is correct, cross-shore and LST sediment transport flux are roughly equivalent, or at least substantial. A number of plots depicting cross-shore and LST sediment transport flux presented by Johnson *et al*. (2010) support this assumption, as does the recent work of Davenport (2020) who has considered tracer experiments driven by a phase resolving model at St Kilda (Figure 4.1).

Reduction or reversal of LST flux associated with islands and reefs structures is observed on the south Otago coast. In terms of coastal geomorphology, the effects of offshore features are relatively well understood and have been simulated for many years in coastal engineering practice as detached breakwaters. The offshore islands and reefs influence mobile coastlines as control points and play an important role in the overall sediment transport regime. This is exemplified best in this study at Waldronville in the lee of Okaihe (Green Island); noting that Ponuiahine (White Island), which comprises a relatively extensive subtidal reef structure, is situated further from the coast than Okaihe, but is considered to have a significant influence on St Clair-St Kilda coastal processes (Allen, 1999; Johnson *et al*., 2010).

Within the St Clair to St Kilda embayment a net sediment flux of almost zero is observed at both Moana Rua Rd and at the Lawyers Head end of the beach. The former is currently subject to aggressive coastal erosion and a priority management area as there is a historical landfill site in this area. The net longshore sediment transport directions are divergent at this site, indicating that it is likely a hinge point, where sediment is transported away in both directions. The work of Johnson *et al.* (2010) indicates that during southerly storm conditions the hinge point would shift further east and likely be more pronounced. The reversal in net sediment transport direction at Lawyers Head is common at many of the headlands along this coast. Duarte et al. (2019) attribute this to wave crest rotation, and it is also common to most headland types under direct (rather than oblique) wave attack (George et al., 2019a).

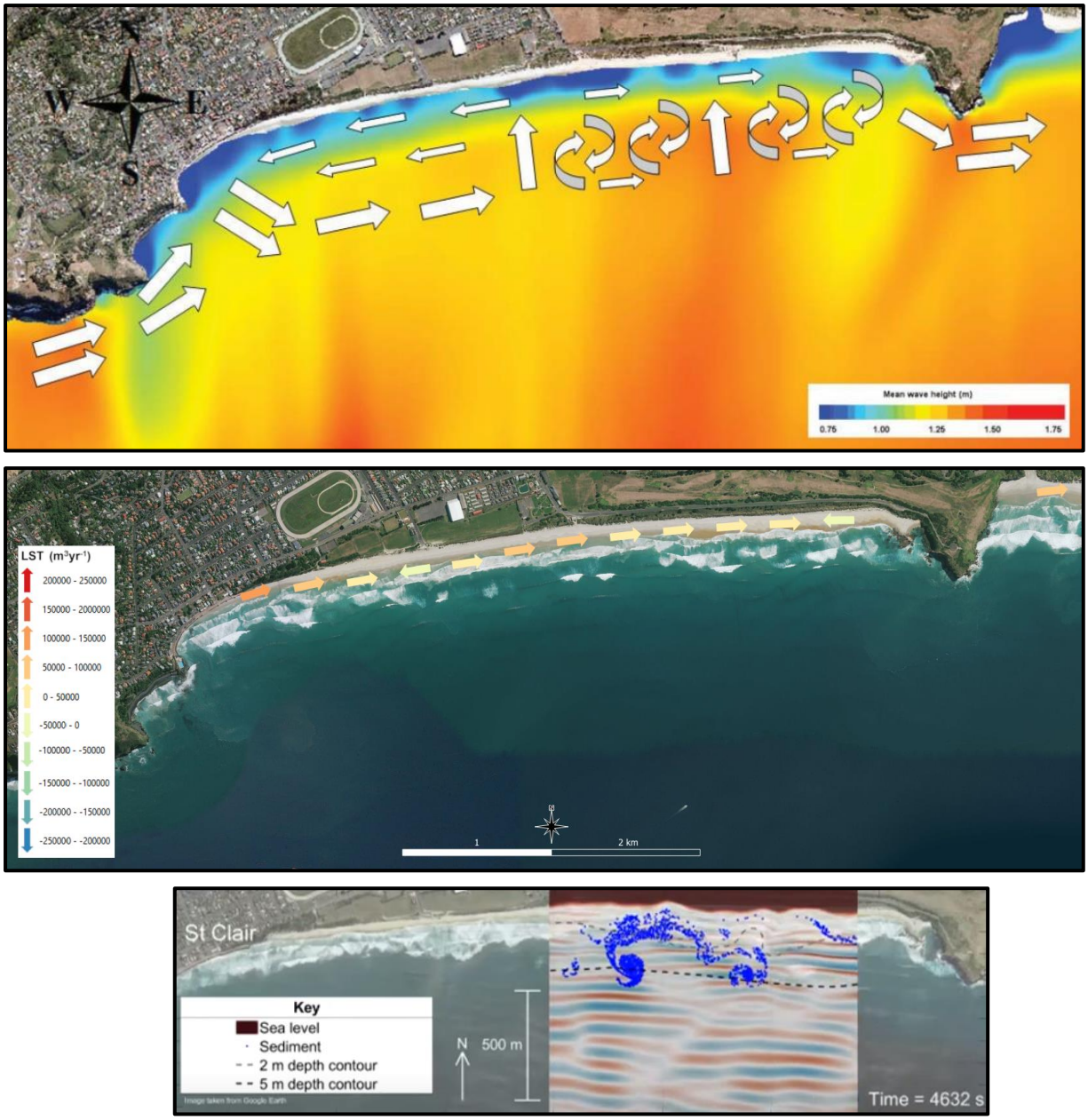

Figure 4.1: Top: Hypothesised sediment transport pathways during southerly storm conditions, along with the annual mean significant wave height (Johnson *et al*., 2010) for St Clair to St Kilda. Middle: LST estimates for the same section of coast. Bottom: tracer experiment driven by a phase resolving model of Davenport (2020) showing cross shore processes.

4.1 Limitations

There are several limitations associated with this modelling exercise:

- This modelling exercise has been undertaken without calibration and validation against recorded *in situ* data (e.g. sediment trapping).
- Reported values for longshore sediment transport flux are valid under the assumption that the material is readily available for transport.
- This work does not account for cross shore transport.

- Wave modelling is dependent on low resolution bathymetric datasets.

4.2 Recommendations

Following the recommendations put forward in the counterpart literature review (Atkin *et al*., 2020), with a view towards the development of a sustainable shoreline management plan for St Clair to St Kilda coast, recommendations for the next steps include:

- Expansion of the historical aerial analysis, including error margins, from 1946 to present to fill in the information gaps between the Toko Mouth/Measley Beach and Waldronville was recommended by Atkin et al. (2020). This information will help to inform and interpret the results of the alongshore sediment transport modelling by further detailing stores and sinks along the coast. While this investigation is still considered useful and would provide further information on the mechanics of the southern Otago sediment transport system, it is not considered a priority for the development of the St Clair to St Kilda long-term management plan.
- A field campaign to validate the transport quantities between Waldronville and St Clair and out of the embayment (i.e. round Lawyer's Head) to provide an understanding of inputs and losses to the beach system in the context of the present findings (i.e. there is very likely a net deficit of sediment input into the southern coast system):
    - Sediment traps/back-scatter measurements
    - Hydrographic transects
    - Wave/current meter deployment
- The sediment transport regime in the St Clair to St Kilda embayment is a function of offshore bathymetry and White Island likely plays a significant role. The bathymetry surrounding White Island appears complex, but it not well resolved, on the nautical chart data used in this study. Given the control point role that offshore islands and reefs play in the hydrodynamic and subsequent morphodynamics of the coastal system, it would be beneficial to the long term aims of developing a coastal plan to have data that justly represents the seafloor adjacent to the St Clair to St Kilda coast. To this end, a bathymetric survey of the features that play an important role in the processes occurring between St Clair and Lawyers Head should be undertaken; which at bare minimum should include verification of charted data across and adjacent to the study site, and high resolution depiction of the reefs and rocky platforms around the St Clair Headland. The latter component of which will be required for an eventual surf break impact assessment study and developing sustainable management strategies.

- Expansion of the existing model to accommodate for high resolution hydrodynamics capable of accounting for the distinct infrastructural and geomorphological differences between St Clair, St Kilda and the Lawyers Head end of the embayment. While a holistic approach should be taken with respect to the management, there are clearly 3 distinct areas of the beach that will likely require different management approaches:

    1. St Clair with its highly modified shoreline including the seawall, swimming pool, geotextile container protection (and associated end-effects) and surfing amenity.
    2. Moana Rua, the central stretch of beach with landfill/contaminated soil in the vulnerable dune area.
    3. The steep St Kilda dune system backed and capped by the John Wilson Ocean Drive.

  Upon determining the preferred adaptation pathway, high resolution numerical modelling supported by field data collection is likely the best way to develop, refine and test long-term solutions for the situation at St Clair due to the complexity of the site. In the absence of these data and information with respect to the local coastal processes, most interventions are likely to be full-scale experiments, which are not recommended due to chance of failure and potential knock-on impacts. The findings of this present study reinforce the likelihood that different approaches will be required for the sustainable management of the different parts of St Clair to St Kilda coast. Consideration of the potential and likely impacts of sea level rise will need to be incorporated into any strategies, which can be achieved through modelling.

References

Allen, C., 1999. Longshore drift at St. Clair Beach and implications for the eroding seawall. Unpublished Post Graduate Diploma Report, University of Otago. 61pps

Atkin, E.A., Mead, S.T. and O'Neil, S., 2020. South Otago Coast Sediment Transport: Literature Summary. eCoast technical report prepared for Dunedin City Council.

Becker, J.J.; Sandwell, D.T.; Smith, W.H.F.; Braud, J.; Binder, B.; Depner, J.; Fabre, D.; Factor, J.; Ingalls, S.; Kim, S-H.; Ladner, R.; Marks, K.; Nelson, S.; Pharaoh, A.; Trimmer, R.; Von Rosenberg, J.; Wallace, G., and Weatherall, P., 2009. Global bathymetry and elevation data at 30 arc seconds resolution: SRTM30_PLUS. Marine Geodesy, 32(4), 355-371.

Brutsché, K.E., Rosati, J., Pollock, C.E. and McFall, B.C., 2016. Calculating Depth of Closure Using WIS Hindcast Data. USACE technical report: ERDC/CHL CHETN-VI-45

Carter, L., 1986. A budget for modern-Holocene sediment on the South Otago continental shelf. New Zealand Journal of Marine and Freshwater Research. 20:4, 665-676, DOI: 10.1080/00288330.1986.9516187

Carter L. and Carter R.M. 1986: Holocene evolution of the nearshore sand wedge, South Otago continental shelf, New Zealand. New Zealand Journal of Geology and Geophysics

Carter R.M., Carter L., Williams J.J., Landis C.A., 1985: Modern and relict sedimentation on the South Otago Continental Shelf, New Zealand. NZ Oceanographic Institute Memoir 93. 43pps.

Davenport, C., 2020. Effects of bathymetry, wave environment and sea level on rip current dynamics in a wave resolving model. Unpublished MSc thesis, University of Otago.

Duarte, J., Taborda, R., Ribeiro, M., 2019. Evidences of headland sediment bypassing at Nazaré Norte Beach, Portugal. In: Proceedings of 9th International Conference in the= Coastal Sediments - Coastal Sediments 2019, Tampa/St. Pete, Florida, pp. 2709–2721. Cited in: Klein, A. H.F. G. Vieira da Silva, R. Taborda, A. P. da Silva, A. D. Short, 2020. Headland bypassing and overpassing: form, processes and applications. Chapter 23, In: Sandy Beach Morphodynamics, Eds. Jackson, D. W. T., and A. D. Short. Elsevier ISBN: 978-0-08-102927-5

Dyer M.J., 1994. Beach profile change at St. Clair Beach, Dunedin. Unpublished MSc thesis, University of Canterbury. 229pps

George, D.A., Largier, J.L., Pasternack, G.B., Barnard, P., Storlazzi, C.D., Erikson, L.H., 2019a. Modeling sediment bypassing around idealized rocky headlands. J. Mar. Sci. Eng. 7, 40, 1-37.Cited in: Klein, A. H.F. G. Vieira da Silva, R. Taborda, A. P. da Silva, A. D. Short, 2020. Headland bypassing and overpassing: form, processes and applications. Chapter 23, In: Sandy Beach Morphodynamics, Eds. Jackson, D. W. T., and A. D. Short. Elsevier ISBN: 978-0-08-102927-5

Gibb, 1979. Late Quaternary shoreline movements in New Zealand. PhD thesis, University of Wellington, New Zealand.

Hallermeier, R.J., 1981. A Profile Zonation for Seasonal Sand Beaches from Wave Climate. Coastal Engineering, 4, 253-277.

Hersbach, H, Bell, B, Berrisford, P, *et al*., 2020. The ERA5 global reanalysis. Q J R Meteorol Soc. 146: 1999– 2049. https://doi.org/10.1002/qj.3803

Hodgson W.A., 1966. Coastal processes around the Otago Peninsula. New Zealand Journal of Geology and Geophysics, 9, 79-90.

Holthuijsen, L.H.; Booij, N.; Ris, R.C.; Haagsma, I.J.G.; Kieftenburg, A.T.T.M.; Kriezi, E.E.; Zijelma, M., and van der Westhyusen, A.J., 2004. SWAN User Manual Cycle III version 40.41. Delft, the Netherlands: Delft University of Technology, 27p.

Johnson, D., McComb, P., Beamsley, B., Weppe, S. and Zyngfogel. R., 2010. Ocean Beach Dunedin - A numerical study of the coastal dynamics. Technical report prepared for Dunedin City Council.

Kalnay, E.; Kanamitsu, M.; Kistler, R.; Collins, W.; Deaven, D.; Gandin, L.; Iredell, M.; Saha, S.; White, G.; Woollen, J.; Zhu, Y.; Leetmaa, A.; Reynolds, R.; Chelliah, M..; Ebisuzaki, W.; Higgins, W.; Janowiak, J.; Mo, K.C.; Ropelewski, C.; Wang, J.; Jenne, R., and Joseph., D., 1996. The NCEP/NCAR 40-year reanalysis project. Bulletin of the American Meteorological Society, 77, 437-470.

Kamphuis, J.W., 1991. Alongshore sediment transport rate. Journal of Waterway, Port, and Coastal, and Ocean Engineering, 117, 624–640.

Kang, H., Chun, I. and Oh, B., 2018. Estimation of Depth of Closure Near Gangneung Port in Korea. Journal of Coastal Research, SI85, 1361-1365.

Fernández-Fernández, S., Baptista, P., Martins, V.A., Silva, P.A., Abreu, T., Pais-Barbosa, J., Bernardes, C., Miranda, P., Rocha, M.V.L., Santos, F., Bernabeu, A. and Rey, D., 2016. Longshore Transport Estimation on Ofir Beach in Northwest Portugal: Sand-Tracer Experiment. Journal of Waterway, Port, Coastal and Ocean Engineering, 04015017.

Mil-Homens, J., Ranasinghe, R., van Thiel de Vries, J.S.M. and Stive, M.J.F., 2013. Re-Evaluation and Improvement of Three Commonly Used Bulk Longshore Sediment Transport Formulas. Coastal Engineering, 75, 29-39.

Serrano, A., 2019. Long Term Coastal Plan for St Clair to St Kilda: Synopsis of Technical Understanding & Data Gap Analysis. Opus technical report prepared for Dunedin City Council

Smith, A.M., 1999. Coastal erosion issues in Otago: Draft sediment budget. Report to Tonkin and Taylor Ltd., Department of Marine Sciences, The University of Otago, 31p.

Smith, A.M., 2000a. Coastal erosion issues in Otago: Past, present, and future. Report to Tonkin and Taylor Ltd. Department of Marine Sciences, The University of Otago, 16p.

Smith, A.M., 2000b. Coastal erosion issues in Otago: Gaps in our knowledge. Report to Tonkin and Taylor Ltd. Department of Marine Sciences, The University of Otago, 9p.

Smith, A.M, 2007. Marine Sedimentation and Coastal Processes on the Otago Coast. University of Otago, Report to Otago Regional Council

Tenzer, R., Sirgueya, P., Rattenbury, M. and Nicolson, J., 2010. A digital rock density map of NewZealand. Computers & Geosciences, 37, 8, 1181-1191.

T&T, 2000. Contact Energy Ltd Clutha Consent Programme Coastal Erosion Issues. Technical Report prepared for Contact Energy Ltd.

Van Rijn, L.C., 2014. A Simple General Expression for Longshore Transport Of Sand, Gravel And Shingle. Coastal Engineering, 90, 23–39.

Williams and Goldsmith, 2014. Coastal morphology of South Otago: Nugget Point to Chrystalls Beach. Otago Regional Council technical report.